

Modelling the ATP production in mitochondria

Alberto Saa

*Departamento de Matemática Aplicada,
Universidade Estadual de Campinas, 13083-859 Campinas, SP, Brazil*

Kellen M. Siqueira

*Instituto de Física “Gleb Wataghin”,
Universidade Estadual de Campinas, 13083-859 Campinas, SP, Brazil*

Abstract

We revisit here the mathematical model for ATP production in mitochondria introduced recently by Bertram, Pedersen, Luciani, and Sherman (BPLS) as a simplification of the more complete but intricate Magnus and Keizer’s model. We correct some inaccuracies in the BPLS original approximations and then analyze some of the dynamical properties of the model. We infer from exhaustive numerical explorations that the enhanced BPLS equations have a unique attractor fixed point for physiologically acceptable ranges of mitochondrial variables and respiration inputs. We determine, in the stationary regime, the dependence of the mitochondrial variables on the respiration inputs, namely the cytosolic concentration of calcium Ca_c and the substrate fructose 1,6-bisphosphate FBP. The same effect of calcium saturation reported for the original BPLS model is observed here. We find out, however, an interesting non-stationary effect: the inertia of the model tends to increase considerably for high concentrations of calcium.

Keywords: Mitochondria, Calcium, ATP, Mathematical model

1. Introduction

The exchange of energy in cells is mostly mediated by ATP (adenosine triphosphate) molecules. Such molecules are produced in several processes in

Email addresses: `asaa@ime.unicamp.br` (Alberto Saa), `kellenms@ifi.unicamp.br` (Kellen M. Siqueira)

an eukaryotic cell, but the principal source of ATP is typically the oxidative phosphorylation process which takes place in mitochondria. The mitochondrion is an organelle with two membranes, having, therefore, two distinct bulk regions: the intermembrane space and the mitochondrial matrix. In the inner membrane, there are plenty of protein transporters and ionic channels, some of which execute an active transport leading to a gradient of some ions and molecules [1, 2]. The metabolic cascade that leads to the production of ATP in the mitochondrion starts in the cytoplasm. At first, glucose is transported from the extracellular medium into the cytoplasm by GLUT transporters. It is then converted in glucose-6-phosphate (G6P) by the enzyme hexokinase. G6P is then converted in pyruvate in a process called glycolysis, in which there is a net production of two ATP molecules. The pyruvate produced is transported into the mitochondrion (to the mitochondrial matrix) and is metabolized in a series of oxidation-reduction reactions in the citric acid cycle leading to the production of the nicotinamide adenine dinucleotide NAD and flavin adenine dinucleotide FAD. These electron donor molecules are oxidized in the complexes I to IV present in the inner mitochondrial membrane. These reactions lead to the activation of a proton pump, creating a pH gradient between the inter membrane space and the matrix. The protons pumped into the intermembrane space return to the matrix through a transporter that uses their energy to catalyze the conversion of ADP (adenosine diphosphate) into ATP. The ATP produced in the mitochondria is then transported to the cytoplasm by the ATP/ADP exchanger [1, 2].

The kinetic aspects of the processes involved in the ATP production in mitochondria are rather intricate. This issue was addressed by Magnus and Keizer (MK), who introduced in the series of papers [3, 4, 5] a theoretical kinetic model for ATP production in mitochondria based on the known biophysical properties of the enzymes and transporters involved in the process. In fact, the MK model was built by considering electrical activity and cytosolic calcium handling in insulin-secreting pancreatic β -cells. The model consists basically in a set of equations describing the dynamics of the citric acid cycle, the proton pump, and the inner mitochondrial membrane transporters of ATP and calcium. The MK model is effectively based on first biophysical principles and provides a very detailed and accurate description of the processes considered to be important for mitochondrial oxidative phosphorylation. However, it is also a rather complex model with cumbersome equations, preventing a systematic mathematical study of its dynamical and physiological properties.

A simplification of the MK model aiming to retain its main dynamical properties was introduced recently by Bertram, Pedersen, Luciani, and Sherman (BPLS) in [6]. The BPLS model incorporates some refinements introduced by Cortassa *et al.* in [7] for the description of the ATP production in cardiac cells. In fact, BPLS model can be considered as an approximation of the Cortassa *et al.*'s model instead of the original MK one. As we will see, this was probably the origin of some inaccuracies in the BPLS equations. As in the original MK model, the mitochondrial ATP production in the BPLS model is governed by four dynamical variables, namely the potential drop in the inner membrane ΔV and the mitochondrial concentrations of: reduced nicotinamide adenine dinucleotide NADH, adenosine diphosphate ADP, and calcium Ca_m . The mitochondrial concentrations of pyridine and adenine nucleotides are assumed to be conserved

$$NAD_m + NADH_m = NAD_{tot}, \quad (1)$$

$$ADP_m + ATP_m = A_{tot}, \quad (2)$$

where NAD_{tot} and A_{tot} stand for the total mitochondrial concentration of the respective nucleotides. The balance of the pertinent fluxes and reactions yields to the following equations

$$\frac{d}{dt}NADH = J_{PDH} - J_0, \quad (3)$$

$$\frac{d}{dt}ADP = J_{ANT} - J_{F1F0}, \quad (4)$$

$$\frac{d}{dt}Ca_m = f_m (J_{uni} - J_{NaCa}), \quad (5)$$

$$\frac{d}{dt}\Delta V = C_m^{-1} (J_H - J_{ANT} - J_{NaCa} - 2J_{uni}), \quad (6)$$

where

$$J_H = J_{H,res} - J_{H,ATP} - J_{H,leak}. \quad (7)$$

The derivation and meaning of the fluxes presented in the right-handed sides of Eq. (3)-(6) are rather involved. The main details and the pertinent references can be found in the BPLS paper [6]. We have checked carefully the derivation of each of these fluxes and we have found out some inaccuracies in the BPLS expressions for adenine nucleotide translocator rate J_{ANT} and for calcium uniporter rate J_{uni} . As we will see, these problems probably have

originated in the transcription of the original MK equations to the Cortassa *et al.*'s model.

In the present paper, we propose some enhanced approximations in the BPLS framework for the fluxes J_{ANT} and J_{uni} and analyze some of the dynamical properties of Eqs. (3)-(6). We show, in particular, that for physiologically acceptable ranges of mitochondrial respiration inputs, namely the cytosolic concentration of calcium Ca_c and the substrate fructose 1,6-bisphosphate FBP, the BPLS equations have a unique physiologically acceptable attractor fixed point. Exhaustive numerical explorations indicate that the BPLS model is indeed globally stable, reinforcing its relevance to physiological quantitative studies, despite its simplicity when compared to the MK original model. We determine, in the stationary regime, the dependence on constant respiration inputs Ca_c and FBP of the of the four mitochondrial variables considered in the model. As in the original BPLS model, we observe here qualitatively distinct behavior for low and high Ca_c concentration excitations. We detect, moreover, a non-stationary effect: the inertia of the model tends to increase considerably for high concentrations of calcium.

2. The Enhanced BPLS Model

We will focus here in the problems for the BPLS expressions for the adenine nucleotide translocator rate J_{ANT} and for calcium uniporter rate J_{uni} , since all the other quantities appearing in (3)-(6) were checked to be correct and accurate for the physiological ranges of variables and parameters. The MK expression for the former is (see Eq. (16) of [3])

$$J_{\text{ANT}} = V_{\text{max,ANT}} \frac{1 - \frac{\text{ATP}_c}{\text{ADP}_c} \frac{\text{ADP}_m}{\text{ATP}_m} e^{-\frac{F\Delta V}{RT}}}{\left(1 + \frac{\text{ATP}_c}{\text{ADP}_c} e^{-f\frac{F\Delta V}{RT}}\right) \left(1 + \frac{\text{ADP}_m}{\text{ATP}_m}\right)}. \quad (8)$$

The precise meaning of all the quantities presented in this formula can be found in [3, 4, 5] or in the BPLS paper [6] as well. On the other hand, the expression for J_{ANT} presented in the Eq. (35) of the Cortassa *et al.* paper [7] lacks the exponential in the numerator as in (8). The BPLS expression for J_{ANT} , obtained probably from Cortassa *et al.*'s Eq. (35), is

$$J_{\text{ANT}} = p_{19} \left(\frac{\frac{\text{ATP}_m}{\text{ADP}_m}}{\frac{\text{ATP}_m}{\text{ADP}_m} + p_{20}} \right) e^{0.5\frac{F\Delta V}{RT}}, \quad (9)$$

where p_{19} and p_{20} are numerical parameters. Notice that Eq. (35) of the BPLS paper has also a mistake in the denominator. The (reasonable) hypothesis used to simplify (8) in the BPLS model is the assumption that, due to the ion transporters action, the rates of ATP to ADP in the mitochondrial matrix and in the cytoplasm are approximately the same,

$$\frac{\text{ATP}_c}{\text{ADP}_c} \approx \frac{\text{ATP}_m}{\text{ADP}_m}. \quad (10)$$

Note that this assumption implies from (8) that $J_{\text{ANT}} \approx 0$ for $\text{ATP}_m \rightarrow \text{A}_{\text{tot}}$ (and, hence, $\text{ADP}_m \rightarrow 0$ according to (2)), which is incompatible with the BPLS expression (9). The same occurs for the limit $\Delta V \rightarrow 0$. With the assumption (10) and taking into account the conservation of mitochondrial pyridine nucleotides (2), the adenine nucleotide translocator rate reads

$$J_{\text{ANT}} = V_{\text{max,ANT}} \frac{\text{ATP}_m}{\text{A}_{\text{tot}}} \frac{1 - e^{-\frac{F\Delta V}{RT}}}{1 + \frac{\text{ATP}_m}{\text{ADP}_m} e^{-f\frac{F\Delta V}{RT}}}. \quad (11)$$

This is our first proposed approximation, which captures all the essential properties of (8) and is simple enough to be mathematically manipulated. Notice that for the typical range of physiological parameters, neglecting the exponential in the numerator of (11) implies an relative error inferior to 5%. We will not, however, adopt this further approximation in this work. Figure (1) illustrate the discrepancies between the expressions (9) and (11) for typical physiological ranges of the parameters and variables. An inspection of the graphics 9(B) of [6] reveals that they have probably compared their approximated expression with their Eq. (35), which was transcribed incorrectly from Cortassa's paper [7].

With respect to the calcium uniporter rate J_{uni} , the original MK expression reads (see Eq. (19) in [3])

$$J_{\text{uni}} = V_{\text{max,uni}} \frac{\frac{2F}{RT}(\Delta V - \Delta V_0)}{1 - e^{-\frac{2F}{RT}(\Delta V - \Delta V_0)}} \frac{\frac{\text{Ca}_c}{K_{\text{trans}}} \left(1 + \frac{\text{Ca}_c}{K_{\text{trans}}}\right)^3}{\left(1 + \frac{\text{Ca}_c}{K_{\text{trans}}}\right)^4 + \frac{L}{(1 + \text{Ca}_c/K_{\text{act}})^{na}}}. \quad (12)$$

In the BPLS derivation of the approximation for J_{uni} , it is used Eq. (38) of Cortassa *et al.* [7], where there is a mistake in the denominator. The BPLS proposed expression for the calcium uniporter rate is

$$J_{\text{uni}} = (p_{21}\Delta V - p_{22})\text{Ca}_c^2, \quad (13)$$

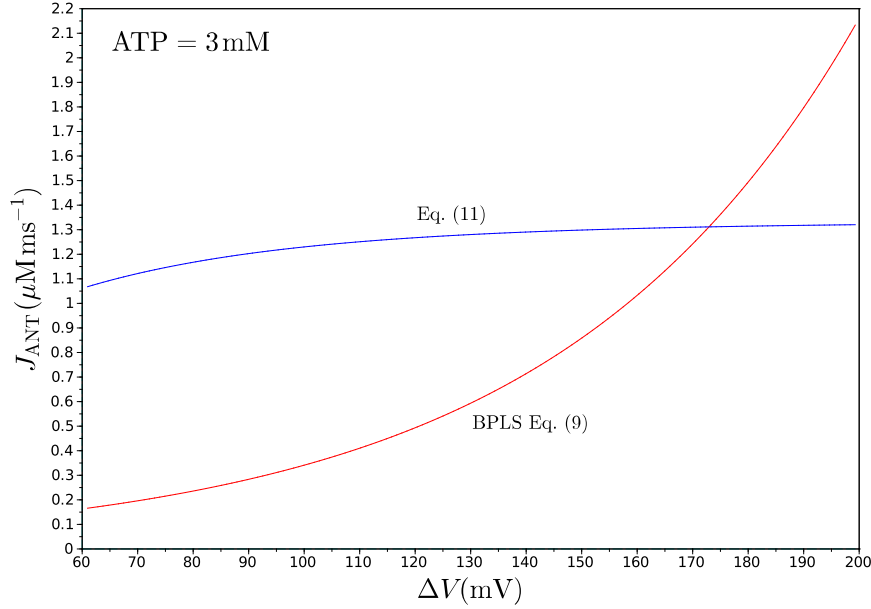


Figure 1: Comparison between the original BPLS expression for the adenine nucleotide translocator rate J_{ANT} (9) and our proposal (11) based on the MK model. Even the concavities of the curves are different. The curves were calculated by assuming $\text{ATP} = 3\text{mM}$ and $A_{\text{tot}} = 15\text{mM}$. An inspection of the graphics 9(B) of [6] reveals that they have probably compared their approximated expression with their Eq. (35), which was transcribed incorrectly from Cortassa's paper [7].

where p_{21} and p_{22} are numerical parameters. We found this equation to be inaccurate for the typical physiological range of parameters. We propose to keep in the approximated model the complete original MK equation (12). Its dependence on ΔV is already in a rather simple form, and the complications for Ca_c are harmless for the dynamical analysis, as we will show. Now, by introducing the following dimensionless variables

$$x = \frac{\text{NADH}_m}{\text{NAD}_{\text{tot}}}, \quad (14)$$

$$y = \frac{\text{ATP}_m}{A_{\text{tot}}}, \quad (15)$$

$$z = \frac{Ca_m}{Ca_0}, \quad (16)$$

$$w = \frac{\Delta V}{\Delta V_0}, \quad (17)$$

$$u = \frac{Ca_c}{Ca_0}, \quad (18)$$

$$v = \frac{FBP}{FBP_0}, \quad (19)$$

where the constant values are presented in Table 1, and taking into account the new proposed expressions (11) and (12), the rates in the right-handed sides of (3)-(6) will be given by

$$J_{PDH} = r_1 \sqrt{v} \frac{z}{a_1 + z} \left(a_2 + \frac{x}{1-x} \right)^{-1}, \quad (20)$$

$$J_0 = r_2 \frac{x}{a_3 + x} (1 + a_4 e^{a_5 w})^{-1}, \quad (21)$$

$$J_{ANT} = r_3 y \frac{1 - e^{-a_6 w}}{1 + \frac{y}{1-y} e^{-a_7 w}}, \quad (22)$$

$$J_{F1F0} = r_4 [(a_8 + y) (1 + a_9 e^{-a_{10} w})]^{-1}, \quad (23)$$

$$J_{H,res} = a_{11} J_0, \quad (24)$$

$$J_{H,ATP} = a_{12} J_{F1F0}, \quad (25)$$

$$J_{H,leak} = r_5 (w - a_{13}), \quad (26)$$

$$J_{NaCa} = r_6 \frac{z}{u} e^{a_{14} w}, \quad (27)$$

$$J_{uni} = r_7 \frac{a_{15}(w-1)}{1 - e^{-a_{15}(w-1)}} G(u), \quad (28)$$

where

$$G(u) = \frac{u(1 + a_{16}u)^{n_a}(1 + a_{17}u)^3}{a_{18} + (1 + a_{16}u)^{n_a}(1 + a_{17}u)^4}. \quad (29)$$

The values of the numerical parameters are presented in Table 1. With the new dimensionless variables, the Eqs. (3)-(6) can be cast in the form

$$\dot{x} = \frac{1}{NAD_{tot}} (J_{PDH} - J_0), \quad (30)$$

$$\dot{y} = \frac{1}{A_{tot}} (J_{F1F0} - J_{ANT}), \quad (31)$$

$\text{NAD}_{\text{tot}} = 10 \times 10^3 \mu\text{M}$	$A_{\text{tot}} = 15 \times 10^3 \mu\text{M}$	$\text{Ca}_0 = 0.2 \mu\text{M}$
$\Delta V_0 = 91 \text{ mV}$	$\text{FBP}_0 = 1 \mu\text{M}$	$C_m = 1.8 \mu\text{M mV}^{-1}$
$V_{\text{max,ANT}} = 5 \mu\text{M ms}^{-1}$	$V_{\text{max,uni}} = 10 \mu\text{M ms}^{-1}$	$\frac{F}{RT} = 0.037 \text{ mV}^{-1}$
$f = 0.5$	$K_{\text{trans}} = 19 \mu\text{M}$	$K_{\text{act}} = 0.38 \mu\text{M}$
$L = 110$	$f_m = 0.01$	$n_a = 2.8$
$r_1 = 0.2 \mu\text{M ms}^{-1}$	$r_2 = 0.6 \mu\text{M ms}^{-1}$	$r_3 = 5 \mu\text{M ms}^{-1}$
$r_4 = 23.3 \mu\text{M ms}^{-1}$	$r_5 = 0.182 \mu\text{M ms}^{-1}$	$r_6 = 0.001 \mu\text{M ms}^{-1}$
$r_7 = 0.11 \mu\text{M ms}^{-1}$		
$a_1 = 0.05$	$a_2 = 1$	$a_3 = 0.01$
$a_4 = 4.23 \times 10^{-16}$	$a_5 = 18.2$	$a_6 = 3.37$
$a_7 = 1.68$	$a_8 = 0.67$	$a_9 = 5.10 \times 10^9$
$a_{10} = 10.7$	$a_{11} = 11.7$	$a_{12} = 3.43$
$a_{13} = 0.16$	$a_{14} = 1.46$	$a_{15} = 6.73$
$a_{16} = 0.52$	$a_{17} = 0.01$	$a_{18} = 110$

Table 1: Numerical parameters and rates for the enhanced BPLS model, see equations (14)-(33). All the values were obtained from [3, 4, 5] and [6].

$$\dot{z} = \frac{f_m}{\text{Ca}_0} (J_{\text{uni}} - J_{\text{NaCa}}), \quad (32)$$

$$\dot{w} = \frac{1}{C_m \Delta V_0} (J_H - J_{\text{ANT}} - J_{\text{NaCa}} - 2J_{\text{uni}}), \quad (33)$$

where f_m and C_m stand, respectively, for the fraction of free Ca ions and the mitochondrial capacitance, see Table 1. Equations (30)-(33) form a non-autonomous systems of four first order differential equations. The external excitations $u(t)$ and $v(t)$ are related, respectively, to the cytosolic concentration of calcium Ca_c and the substrate fructose 1,6-bisphosphate FBP, see Eqs. (18) and (19). We can now start the dynamical analysis of the model.

3. Dynamics of the model

Let us consider initially the fixed points (x_*, y_*, z_*, w_*) of the system (30)-(33) assuming constant inputs (u_*, v_*) . The physiologically meaningful range for the variables x and y is $[0, 1]$ by construction, see (1)-(2) and (14)-(15). For z and w , we assume only that they are non negative. The typical physiological range for the potential drop, however, is more restrictive, corresponding to $\Delta V \approx [90, 225] \text{ mV}$, which is equivalent to $w \approx [1, 2.5]$. For the inputs u and v , we consider the ranges $[0, 10]$ and $[0, 20]$, respectively,

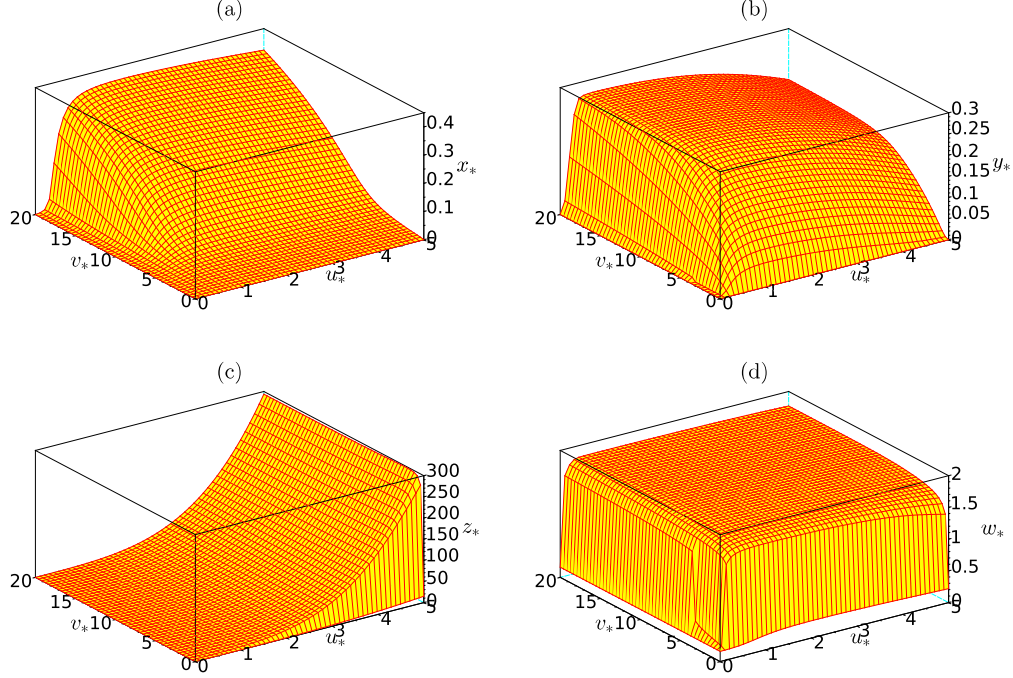


Figure 2: The globally stable physiological fixed point (x_*, y_*, z_*, w_*) of the system (30)-(33) assuming constant inputs (u_*, v_*) .

which corresponds to $\text{Ca}_c \approx [0, 2] \mu\text{M}$ and $\text{FBP} \approx [0, 20] \mu\text{M}$. We perform an exhaustive numerical search [8] for fixed points of (30)-(33) by assuming $u \in [0, 10]$ and $v \in [0, 20]$ constants. For all tested values of u and v , only one physiological ($x, y \in [0, 1]$ both $z, w > 0$) fixed point was found, which is always stable. Moreover, the fixed point is globally stable for physiological ranges of variables, meaning that any solution of (30)-(33) with reasonable initial conditions will tend asymptotically to the fixed point. The variable w and x have the quickest convergence to the fixed point, where y and z are the slowest ones. The values of (x_*, y_*, z_*, w_*) as function of the constant inputs (u_*, v_*) are depicted in Fig. (2), from where one can already observe some physiologically consistent dynamical properties which we describe briefly below.

First, the production of ATP and the concentration of NADH vanishes in the absence of cytosolic calcium Ca_c and/or the substrate fructose 1,6-bisphosphate FBP, *i.e.*, x and $y \rightarrow 0$ for u or $v \rightarrow 0$. Also, we see that for

reasonable values of u and v the value of the potential drop ΔV (w) is almost constant and close to 150 mV. This stability is probably the reason why the original BPLS model is robust, despite the inaccuracies for the expression of J_{ANT} and J_0 we are correcting in this paper. We will return to this point in the last section.

Another important feature of the BPLS model is the reversion of some mitochondrial variables dynamical behavior in the presence of lower and higher concentration of calcium, which can be simulated, as described in [6], by setting $a_1 = 0$ in the expression for J_{PDH} (20). This conclusion can be inferred from Fig. 2, but it is better illustrated in Fig. 3, which depicts the solutions of (30)-(33) for an oscillatory Ca_c input of the form

$$u(t) = u_0 + u_1 \sin(t/t_0), \quad (34)$$

with constant $v(t)$ and initial conditions $(x(0), y(0), z(0), w(0))$ given by the values of the fixed point corresponding to $u_* = u(0)$ and $v_* = v(0)$. As we will see, such a choice of initial condition is consistent with the adiabatic regime we observe for sufficiently slow inputs (large period t_0). For lower values of u_0 (low Ca_c concentrations), all the mitochondrial variables increases and decreases in synchrony with the variations of u . On the other hand, for higher values of u_0 , the dynamical behavior of x , y and w is reversed. *i.e.*, they tend to decrease/increase while u increases/decreases. This effect can be understood from the relation between u_* and z_* depicted in Fig. 2.c. The value of z_* tends to increase rapidly when u_* increases, and this behavior can be traced back to the condition $J_{\text{NaCa}} = J_{\text{uni}}$ defining the fixed point $\dot{z}_* = 0$. However, for large values of z , the dependence of the expression for J_{PDH} (20) on z saturates and becomes equivalent to setting $a_1 = 0$. Without the z suppression term in J_{PDH} , the dynamical behavior of the variables x , y , and w is reversed, as it was pointed out in the original BPLS analysis. The value of v (FBP) does not change qualitatively this dynamical behavior.

The oscillatory excitations illustrated in Fig. 3 has period $t_0 = 3$ min. For inputs varying over a time scale of minutes, the system evolves adiabatically in a good approximation, *i.e.*, the instantaneous solution $(x(t), y(t), z(t), w(t))$ is well approximated by the fixed point (x_*, y_*, z_*, w_*) corresponding to $u_* = u(t)$ and $v_* = v(t)$. In other words, for slowly varying inputs, the solutions of the system are confined to the fixed-point surfaces depicted in Fig. 2. Of course, one expects a breakdown of this adiabatic behavior for rapidly varying inputs. Non-stationary effects must appear for inputs varying with

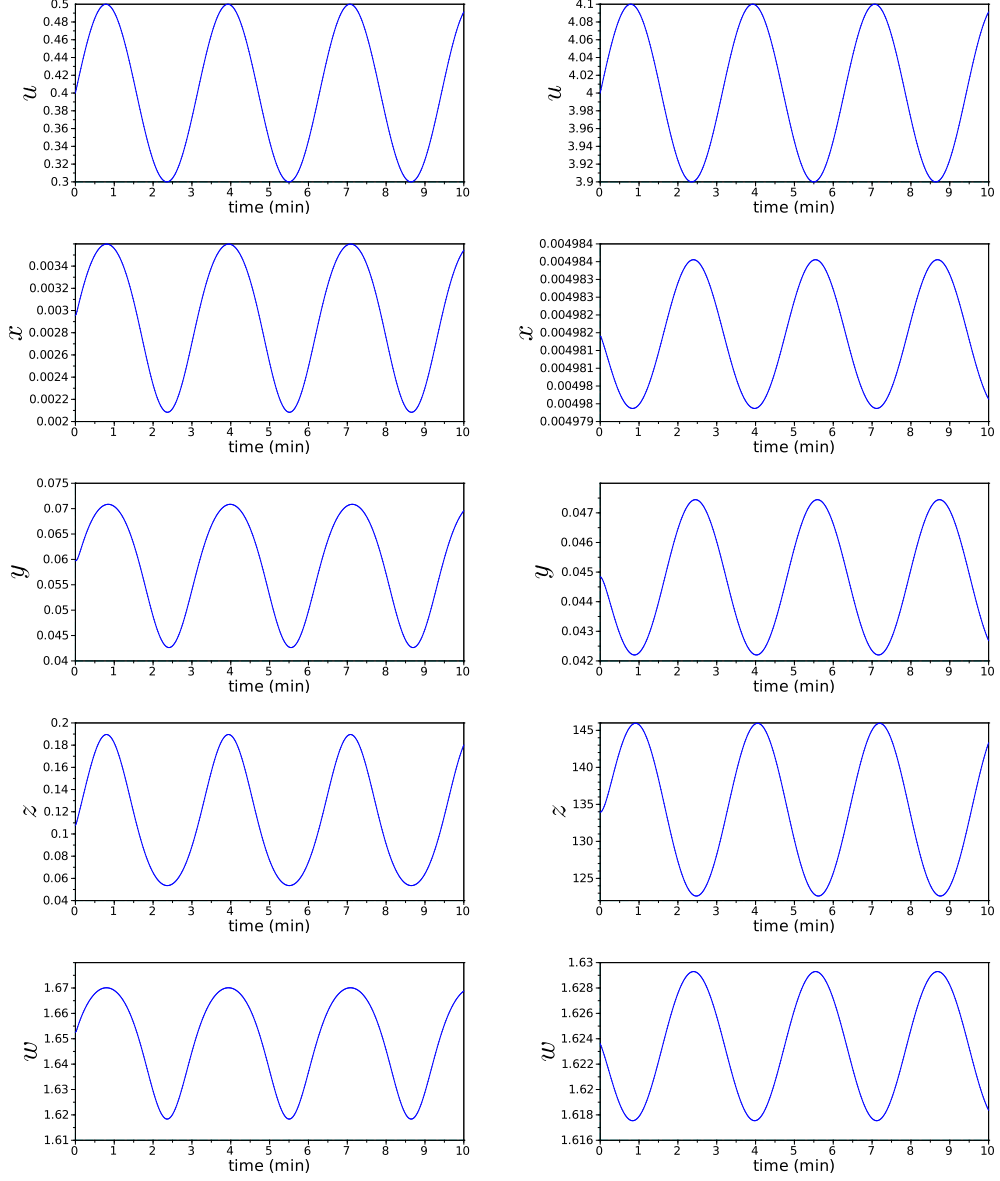


Figure 3: Response of the equations (30)-(33) to oscillatory inputs (34). Notice that for low Ca_c concentrations, all the mitochondrial variables increases and decreases in synchrony with the variations of u . On the other hand, for high Ca_c concentrations, the behavior of x , y and w is reversed. All the curves were evaluated for $\text{FBP} = 0.5 \mu\text{M}$. See the text for further details.

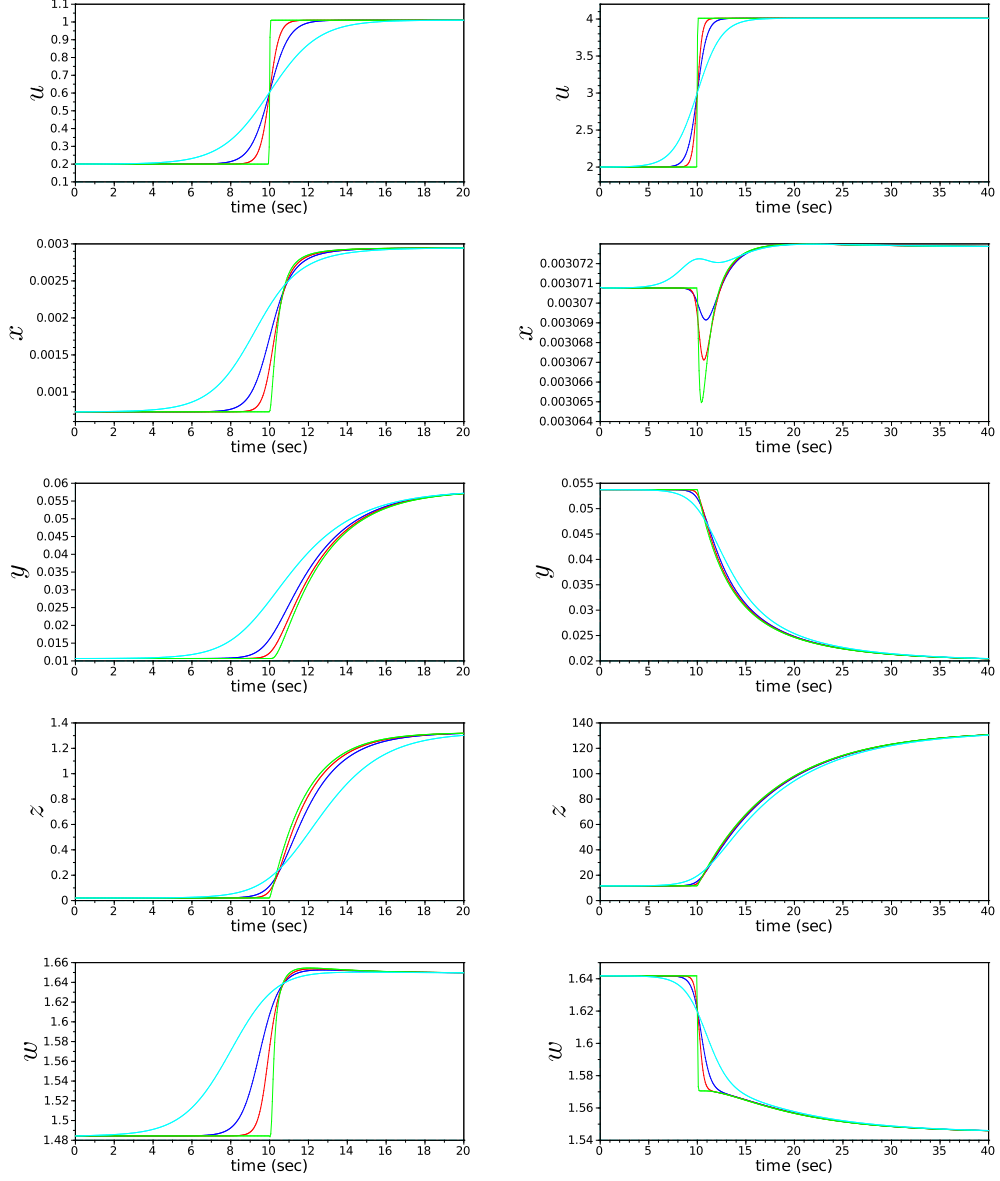


Figure 4: Response of the equations (30)-(33) to step-like inputs (35). The inertia of the system increases considerably for higher values of u , see the text for further details. The curves were evaluated for $\text{FBP} = 0.5 \mu\text{M}$.

a characteristic time smaller than a certain critical value. In order to study non-stationary effects, we consider the response of the system for inputs of

the type

$$u(t) = u_0 + u_1 \tanh(t/t_0), \quad (35)$$

for different values of t_0 . This situation is depicted in Fig. 4 for some values of u_0 and u_1 and for $t_0 = 2.5, 1, 0.5$, and 0.02 seconds. It is clear that for lower values of u (Ca_c), approximately 10 seconds are enough to assure that the system reaches an adiabatic regime. As we have already noticed, the variables y (ATP) and z (Ca_m) are the slowest ones to attain their respective stationary regime. Increasing the values of u implies the increasing of such “relaxation” time. The second column in Fig. 4 corresponds to a situation with $u \in [2, 4]$, for which almost 30 seconds are necessary to assure the attainment of the stationary regime. The inertia of the system, hence, increases considerably for higher concentrations of cytosolic calcium.

4. Final Remarks

We have revisited here the mathematical model for ATP production in mitochondria introduced recently by Bertram, Pedersen, Luciani, and Sherman (BPLS) in [6] as a simplification of the more complete but intricate Magnus and Keizer’s model [3, 4, 5]. We checked carefully all the approximations introduced in the BPLS model and found some inaccuracies for the approximations used for the adenine nucleotide translocator rate J_{ANT} and for calcium uniporter rate J_{uni} . We proposed enhanced approximations for such rates based on the original Magnus and Keizer’s model and analyzed some dynamical properties of the model. Our results for the stationary regime indicate that the BPLS model is indeed globally stable, reinforcing its relevance to physiological quantitative studies, despite its simplicity when compared to the Magnus and Keizer’s model. We have considered also the non-stationary regime and detected an interesting effect: the inertia of the model tends to increase considerably for high concentrations of cytosolic calcium.

It is interesting to notice that the dynamics of our enhanced model are qualitatively similar to the original BPLS one, despite the differences in the rates J_{ANT} and J_{uni} for physiological ranges, as depicted, for instance, in Fig. 1. This point can be understood from the fact that the value of w_* , which does not depends tightly on the details of such rates, is almost constant and corresponding to $\Delta V = 150 \text{ mV}$ for reasonable values of the inputs v_* and u_* . For a fixed value of ΔV , the numerical parameters in (9) can be

fitted to provide a good adjustment for the real ATP dependence of (11). An inspection of Fig. 9 of [6] reveals that the adjustment of their numerical parameters was checked for $\Delta V \approx 160$ mV, which is close to the physiological fixed point.

Acknowledgements

The authors are grateful to FAPESP and CNPq for the financial support.

References

References

- [1] A. C. Guyton and J. E. Hall, Textbook of Medical Physiology, Elsevier (2006).
- [2] D. L. Nelson and M. Cox, Lehninger Principles of Biochemistry, W. H. Freeman and Company (2004).
- [3] G. Magnus and J. Keizer, Am. J. Physiol. **273**, C717-C733 (1997).
- [4] G. Magnus and J. Keizer, Am. J. Physiol. **274**, C1158-C1173 (1998).
- [5] G. Magnus and J. Keizer, Am. J. Physiol. **274**, C1174-C1184 (1998).
- [6] R. Bertram, M.G. Pedersen, D.S. Luciani, and A. Shermand, J. Theor. Biol. **243**, 575-586 (2006).
- [7] S. Cortassa, M.A. Aon, E. Marban, R.L. Winslow, and B. O'Rourke, Biophys. J. **84**, 2734-2755 (2003).
- [8] Scilab files are available at <http://vigo.ime.unicamp.br/atp>